TÜBİTAK

Turkish Journal of Chemistry

http://journals.tubitak.gov.tr/chem/

Research Article

Turk J Chem
(2018) 42: 291 – 305

doi:10.3906/kim-1704-21

Voltammetric determination of vanillin in commercial food products using overoxidized poly(pyrrole) film-modified glassy carbon electrodes

Şükriye ULUBAY KARABİBEROĞLU[1,*], **Çağrı Ceylan KOÇAK**[2]

[1]Department of Chemistry, Faculty of Science, Ege University, Bornova, İzmir, Turkey

[2]Department of Occupational Health and Safety, Bergama Vocational School, Dokuz Eylül University, İzmir, Turkey

Received: 12.04.2017 • **Accepted/Published Online:** 26.09.2017 • **Final Version:** 27.04.2018

Abstract: In this work, a very simple, rapid, cheap, sensitive, and selective polymer film-modified electrode for vanillin determination in commercial food products was developed via electrochemical polymerization and overoxidation of pyrrole. The formation of both poly(pyrrole) and overoxidized poly(pyrrole) films on a glassy carbon electrode surface was characterized by electrochemical impedance spectroscopy, scanning electron microscopy, and X-ray photoelectron spectroscopy. Under optimized conditions, the calibration graph comprises two linear segments of 0.032–1.500 μmol L^{-1} and 3.00–150.00 μmol L^{-1} with a detection limit of 0.012 μmol L^{-1}. The selectivity of the modified electrode was examined in the presence of metals, inorganic ions, and organic substances. Moreover, the proposed method was successfully used for the assessment of vanillin contents in commercial food products with satisfactory results.

Key words: Polymer film electrode, overoxidized polymer, vanillin determination

1. Introduction

The main chemical component of natural vanilla is vanillin (VAN; 4-hydroxy-3-methoxybenzaldehyde), which is extensively used as a flavoring in confectionery, tobaccos, beverages, foods, pharmaceuticals, and perfumes. The reason for the widespread use of VAN is its desirable flavor and aroma properties.[1–3] Synthetic VAN is extensively used as an additive due to the high-cost production of natural VAN from vanilla beans or pods.[4]

VAN also has positive health effects such as preventing cardiac disease mortality, antisickling influence in sickle cell disease, and defending human keratinocyte stem cells against ultraviolet B irradiation.[5–7] However, excessive consumption of synthetic VAN can cause some side effects such as headache, nausea, vomiting, and allergic reactions, and it can also cause damage to the liver and kidneys.[8–11] Hence, for the sake of food safety and quality, it is crucial to develop an approach for simple, sensitive, and low-cost determination of VAN concentrations in foodstuff.

Several analytical methods can be used for the analysis of VAN such as gas chromatography,[12,13] high-performance liquid chromatography,[14,15] spectroscopy,[16] and capillary electrophoresis.[17] Although satisfactory results have been obtained using these sensitive methods, they have disadvantages including time-consuming procedures, complicated pretreatment, and high-cost analysis equipment.[6,11,18] On the other hand, other alternative techniques for VAN determination are electroanalytical methods, which are simple, cheap, rapid, sensitive, and selective. Despite these advantages, electrooxidation of VAN at bare electrodes occurs at a relatively high

*Correspondence: sukriyeulubay@gmail.com

potential, and the sensitivity and selectivity are inadequate due to a fouling effect or the electrooxidation of VAN, which is phenolic compound that can produce phenoxy radicals that readily polymerize and passivize the electrode surface.[5] The most effective way of overcoming this problem is to modify the surface of bare electrodes with various materials such as graphene, polymers, metal nanoparticles, and carbon nanotubes, which have fascinating structures and low price. Examples of electrodes modified with these materials for VAN determination are acetylene black paste electrodes modified with graphene–polyvinylpyrrolidone composite films,[19] glassy carbon electrode (GCE) modified with gold nanoparticles stabilized in poly(allylamine hydrochloride),[20] electrolytic manganese dioxide–graphene composite-modified electrode,[8] cobalt sulfide nanorods–Nafion-modified GCE,[21] poly(valine)-modified GCE,[10] poly(acid chrome blue K)-modified GCE,[7] Ag nanoplates–graphene composite,[22] Au–Ag alloy nanoparticle-modified GCE,[2] Au–Pd nanoparticles–graphene composite-modified GCE,[9] poly(Alizarin Red-S)-modified GCE,[3] and molecularly imprinted ionic liquid polymer–carboxyl single-walled carbon nanotube composite electrode.[18]

Recently, conducting polymers have attracted much interest and have been widely used in electroanalytical applications because of their high conductivity, easy synthesis, and low-cost processability.[3,23,24] A common method of polymer film synthesis on electrode surfaces is electropolymerization due to its advantage of forming reproducible polymer films with controllable film thickness.[25] To improve the conductivity and obtain more porous surfaces, polymer films should be overoxidized at high potentials. Poly(pyrrole), which is an attractive polymer due to its commercial availability, ease of oxidation, high chemical stability, and high electronic conductivity, is positively charged when it is oxidized at high positive potentials. As a result of overoxidation of poly(pyrrole), additional carbonyl and carboxyl groups can appear in the polymeric structure.

To our knowledge, there has been no paper published about VAN determination at overoxidized poly(pyrrole)-modified GCEs. In this study, an overoxidized poly(pyrrole)-modified glassy carbon electrode was prepared to develop a simple and sensitive method for VAN determination. For this purpose, after the poly(pyrrole) electrode was fabricated at the GCE electrode surface via electrochemical polymerization by cyclic voltammetry, overoxidation of the polymer film was carried out using a chronoamperometric technique. The modified electrodes were characterized using electrochemical impedance spectroscopy (EIS), X-ray photoelectron spectroscopy (XPS), and scanning electron microscopy (SEM) techniques. The overoxidized polymer film electrode (PPy_{ov-ox}/GCE) was also used for VAN determination in commercial food products.

2. Results and discussion

2.1. Electrochemical preparation and characterization of PPy films and PPy_{ov-ox} on GCE surface

Figure 1A displays the cyclic voltammograms of poly(pyrrole) film formation on the GCE surface. The electrode potential was scanned seven times between –0.35 and 0.85 V at a scan rate of 20 mV s^{-1} in 0.1 mol L^{-1} pyrrole dissolved in 0.1 mol L^{-1} sodium dodecyl sulfate. No oxidation or reduction peaks were observed during the first potential scan. An irreversible oxidation peak occurred at about 0.1 V during the 4th cycle. During the successive potential sweep, the oxidation peak current increases, indicating that the conductivity of the electrode surface increases. To enhance the electrochemical reactivity of the PPy/GC electrode, the overoxidation process was accomplished in NaOH solutions at a constant potential (Figure 1B). As can be seen from Figure 1B, the current suddenly decreases after 60 s and reaches a stable value at 80 s. As a result of the overoxidation step, gain-enhanced conductivity and a more porous surface due to the formation of carbonyl and carboxyl groups were obtained by chronoamperometry.[26–29]

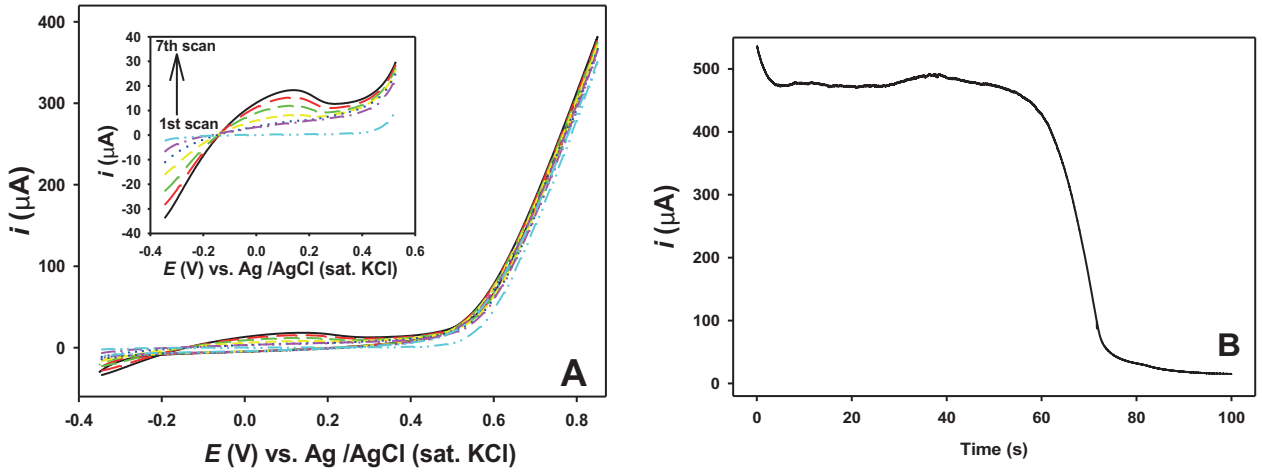

Figure 1. A) Cyclic voltammograms of 0.1 mol L^{-1} pyrrole polymerization on a GCE electrode in 0.1 mol L^{-1} SDS from 1st cycle to 7th cycle. Inset: Magnified oxidation peak. B) Overoxidation of poly(pyrrole) at 1.0 V on GCE in 0.1 M NaOH solution.

To examine the interfacial electrical properties of bare and modified GC electrodes, EIS measurements were performed in 0.1 mol L^{-1} KCl solution containing 5 mmol L^{-1} $K_3[Fe(CN)_6]/K_4[Fe(CN)_6]$. EIS studies provide valuable information about the charge transfer resistance (R_{ct}) between electrode and electrolyte interfaces and the electrical conductivity of all electrodes. An impedance spectrum comprises two parts, which are a semicircular part at high frequencies related to the electron-transfer process and a linear region at low frequencies indicating diffusion-controlled electrode reactions. The R_{ct} value is proportional to the semicircle radius in a Nyquist plot and it gives information about the conductivity of the electrodes. Figure 2 shows the Nyquist plots for bare, PPy-, and PPy_{ov-ox}-modified GC electrodes. R_{ct} and other component values, the ohmic resistance of the electrolyte solution (R_s), double-layer capacitance (C_{dl}), electron-transfer resistance (R_{ct}), and Warburg impedance (W) were obtained from EIS measurements by fitting data using a Randles equivalent circuit model. The R_{ct} values of bare, PPy-, and PPy_{ov-ox} modified GC electrodes are 343 Ω, 671 Ω, and 168 Ω, respectively. The highest R_{ct} value was obtained with the PPy-modified GC electrode, which indicates that the conductivity was decreased by modification of the GC electrode surface with the polymer film. The R_{ct} value decreased due to overoxidation of the PPy film. The low R_{ct} value for PPy_{ov-ox}/GCE suggests that the charge transfer process is relatively fast compared with the other two electrodes and the conductivity of the PPy/GC electrode is greatly enhanced with the overoxidation step. The R_s values were measured as 202 Ω, 204 Ω, and 207 Ω for bare GCE, PPy/GCE, and PPy_{ov-ox}/GCE. This negligible difference in R_s values indicates that the ohmic resistance of the solution is not influenced by electrode modification. The highest Warburg impedance value was observed with the PPy_{ov-ox}/GC electrode because more ions linearly diffused from the solution to the electrode surface. The C_{dl} value is increased with the PPy_{ov-ox}/GC electrode (2.82 μF for bare GCE, 1.43 μF for PPy/GCE, and 4.25 μF for PPy_{ov-ox}/GCE), which is probably because electron transfer becomes easier when the electroactive surface area is increased. These results imply that the PPy_{ov-ox}/GC electrode has good conductivity, which facilitates the electron transfer.

The Randles–Sevcik equation (Eq. (1)) was used to test whether the electroactive surface area of the modified electrodes[30,31] was increased in 1.0 mmol L^{-1} $K_4Fe(CN)_6$ + 0.1 mol L^{-1} KCl solution:

$$I_p = \left(2.69 \times 10^5\right) n^{3/2} A D^{1/2} C^* v^{1/2} \quad (1)$$

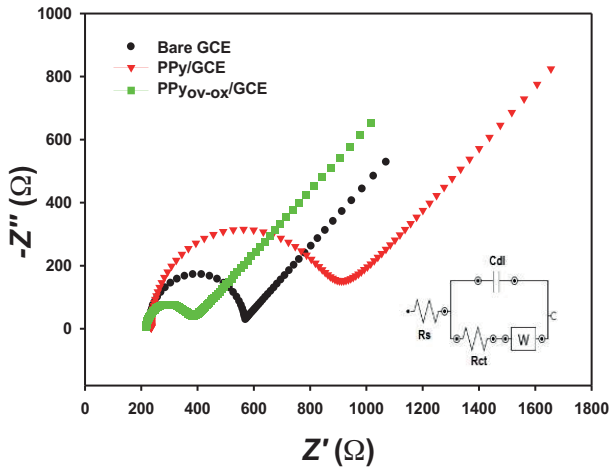

Figure 2. Nyquist plots of bare GCE (●), PPhRed/GCE (▼), and PPhRed$_{ox}$/GCE (■) in 0.1 M KCl solution containing 5 mM $K_3[Fe(CN)_6]/K_4[Fe(CN)_6]$. Frequency range: 100 mHz to 100 kHz, amplitude: 10.0 mV. Inset: Equivalent electrical circuit.

In this equation, n denotes the number of electrons transferred in the redox reaction (n = 1), v is the scan rate of the potential sweep (V/s), A is the electroactive surface area (cm^2), D is the diffusion coefficient of the molecules in the solution (D = 6.7 × 10^{-6} cm^2 s^{-1} at 25 °C), C* is the concentration of $K_4Fe(CN)_6$ (1.0 mmol L^{-1}), and I_p is the peak current of the redox couple[32] From the slope of a linear plot of I_p vs. $v^{1/2}$, the electroactive surface areas of bare GCE, PPy/GCE, and PPy$_{ov-ox}$/GCE were calculated as 0.0485, 0.0945, and 0.2819 cm^2, respectively. Clearly, after overoxidation of the PPy film, the electroactive surface area was increased due to the formation of more functional carbonyl and carboxyl (-COO^-/COOH) groups on the polymer film surface, which is in good agreement with the XPS data (Figure 4).

SEM measurements were performed in order to examine the surface morphologies of PPy/GCE and PPy$_{ov-ox}$/GCE and to monitor the surface characteristics. Figure 3A shows an SEM image of the PPy/GCE surface; the film has a homogeneous porous surface with small microspherical grains. On the other hand, as can be seen from Figure 3B, after overoxidation of the polymer film, the surface porosity was increased due to formation of additional functional groups (-COO^-/-COOH).

XPS measurements were performed to evaluate the chemical compositions of PPy/GCE and PPy$_{ov-ox}$/GCE surfaces. Figures 4A and 4B display detailed C1s and N1s spectra relevant to PPy/GCE and PPy after overoxidation. The curve fits of the C1s peaks for PPy and PPy$_{ov-ox}$ include three components located at 284.27, 284.75, and 285.78 eV and 284.31, 285.01, and 286.06 eV, respectively (Figure 4A). Signals at low energies (located at 284.27 eV and 284.31 eV) are generally associated with C=C (sp^2) bonding in polymeric rings. The other signals centered at 284.75 eV and 285.01 eV are attributed to C–C (sp^3) and C–N bonding, respectively, in PPy and PPy$_{ov-ox}$ polymeric structures.[33–35] As expected, a new peak located at 287.37 eV was observed after overoxidation of the PPy film. This new peak is associated with COOH/COO^- functionalities in PPy$_{ov-ox}$.[33,36] The fitted N1s spectra of PPy and PPy$_{ov-ox}$ surfaces are shown in Figure 4B. The N1s peak has four main components located at 397.98 eV, 399.49 eV, 400.00 eV, and 401.55 eV. The peak at 399.49 eV is assigned to neutral amine nitrogen (–NH–) and the higher binding energy components centered at 400.00 eV and 401.55 eV are assigned to positively charged amine nitrogens (polarons and bipolarons, respectively) in

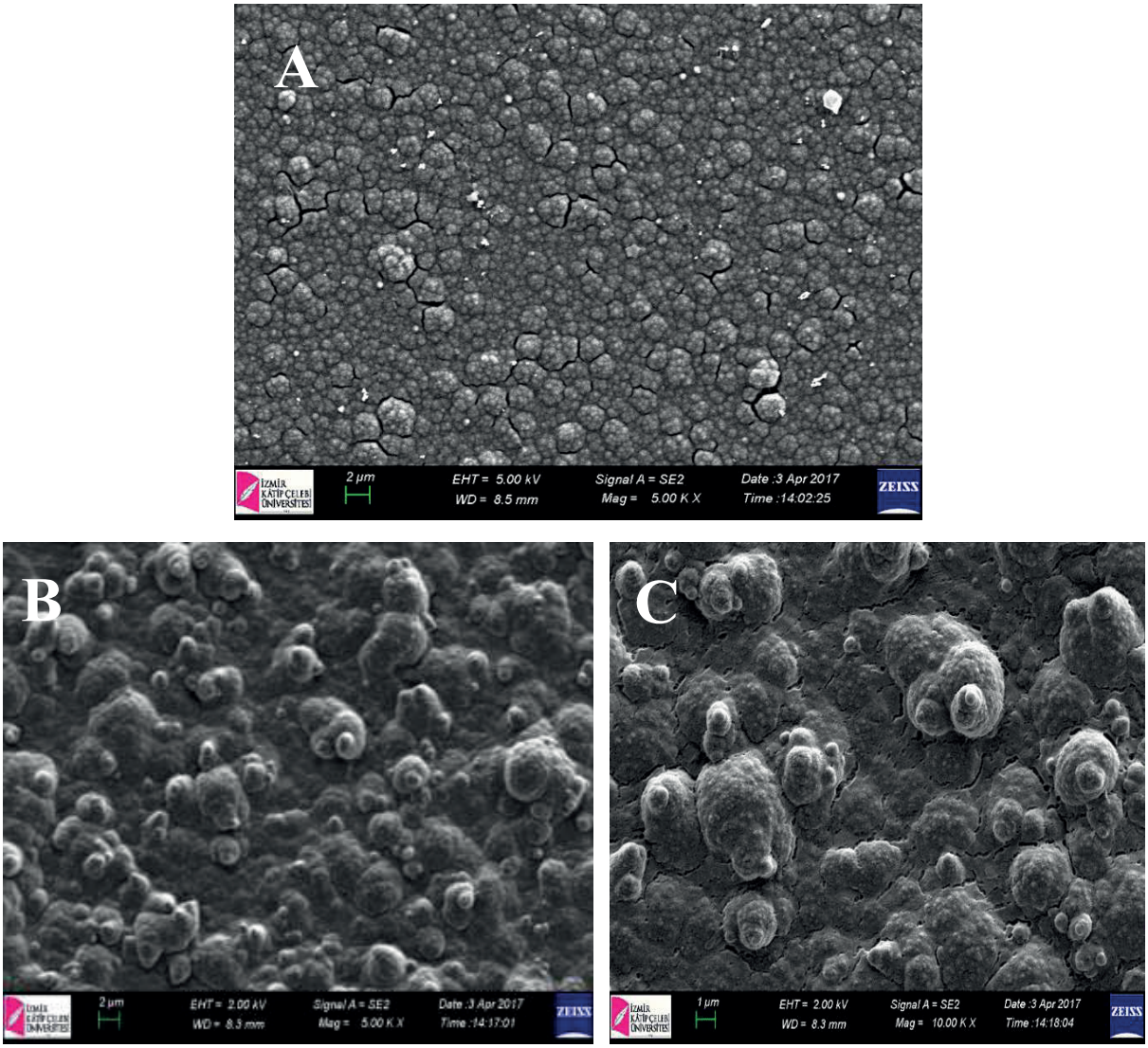

Figure 3. SEM images of A) PPy/GCE, B) PPy$_{ov-ox}$/GCE (5000× magnitude), and C) PPy$_{ov-ox}$/GCE (10,000× magnitude) film on GCE with different magnitudes.

PPy. In the case of PPy$_{ov-ox}$/GCE, the peak at 397.88 eV can be attributed to the =N–bonds in overoxidized polymer rings. The peaks at 399.73 eV and 400.13 eV can be attributed to NH$^{\delta+}$. The presence of NH$^{\delta+}$ indicates that PPy is partially overoxidized.[36–38]

2.2. Electrochemical oxidation of VAN on different electrodes

Figures 5A and 5B display cyclic voltammograms (CVs) of the absence or presence of 0.1 mmol L^{-1} vanillin on bare GCE, PPy/GCE, and PPy$_{ov-ox}$/GCE surfaces in pH 5.2 acetic acid/acetate buffer solution. Clear background signals were obtained in the absence of VAN (Figure 5A) for the bare and modified electrodes in the studied potential range. As is clearly seen from Figure 5A, the background current increased with electrode modification with poly(pyrrole) due to the increasing of the electrode surface area. With addition

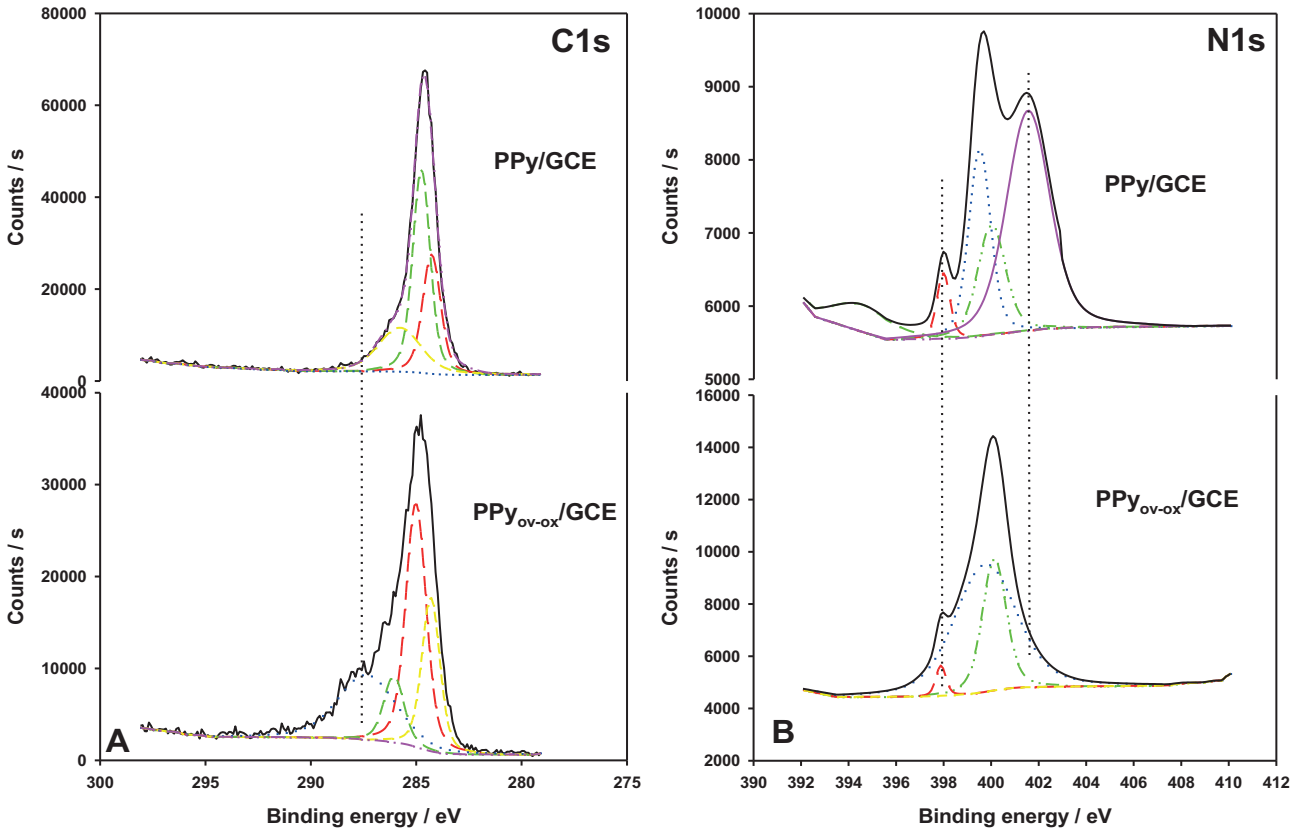

Figure 4. XPS detailed spectra of A) C1s and B) N1s of PPy/GCE and PPy$_{ov-ox}$/GCE.

of 0.1 mmol L^{-1} vanillin into the pH 5.2 acetic acid/acetate buffer solution (Figure 5B), an irreversible peak of VAN electrooxidation was observed at 0.73 V with a small peak current on bare GCE; the oxidation peak of VAN disappeared on PPy/GCE due to the decreased conductivity caused by poly(pyrrole) modification on GCE surface, and the background current increased significantly. On the other hand, the oxidation peak of VAN was obtained at 0.79 V and the peak current dramatically increased by about 12.0 times on PPy$_{ov-ox}$/GCE compared with bare GCE. The increase in the peak current for 0.1 mmol L^{-1} VAN confirms the overoxidation of the PPy/GCE surface, which means that the formation of -COO$^-$ and COOH groups on PPy surface catalyzed the oxidation of VAN.

To find optimum conditions for VAN determination, some main parameters associated with preparation of the overoxidized PPy film and supporting electrolytes during the polymerization step were also examined. The concentration of pyrrole monomer, cycle number of the electropolymerization step, scan rate of electropolymerization potential scan, time and potential of the overoxidation process, and NaOH concentration were chosen as parameters that could be optimized for overoxidized PPy film preparation. These parameters were readily determined by evaluating the peak current of VAN oxidation and the optimized parameters were obtained as follows: 0.1 mol L^{-1} pyrrole; seven cycles for electropolymerization; 20 mV s^{-1} scan rate; 100 s and 1.0 V as overoxidation time and potential, respectively; and 0.1 mol L^{-1} NaOH.

2.3. The effect of supporting electrolyte pH on VAN electrooxidation

The effect of pH on the oxidation of 0.1 mmol L^{-1} VAN was studied in the whole pH range used (3.15–9.13) by linear voltammetry on PPy$_{ov-ox}$/GCE (Figure 6A). In Figure 6B, the highest oxidation peak currents are

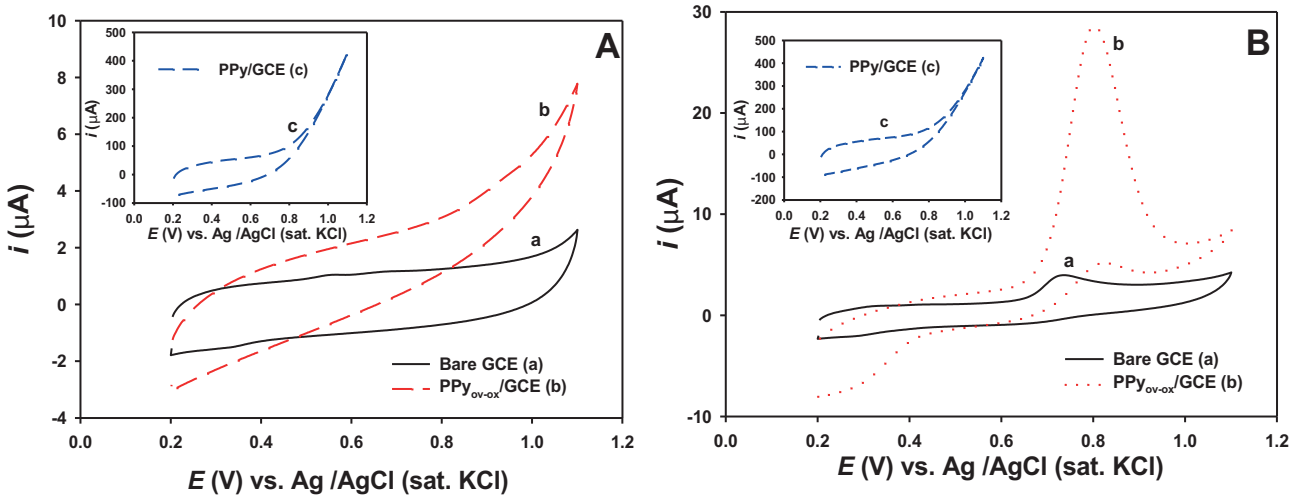

Figure 5. Cyclic voltammograms in the absence (A) and in the presence (B) of 0.1 mmol L^{-1} VAN at a bare GCE (a), PPy_{ov-ox}/GCE (b), and PPy/GCE (c- inset of Figures 5A and 5B) in 0.1 M pH 5.2 buffer solution, with scan rate 50 mV s^{-1}.

obtained with pH 5.2 buffer solution. Thus, the subsequent electrochemical measurements were performed in 0.1 mol L^{-1}, pH 5.2 buffer solution. It was also found that the peak potential of VAN electrooxidation on PPy_{ov-ox}/GCE shifted to negative potential values with increasing pH (Figure 6B), which proved that protons were directly involved in the VAN electrooxidation. The peak potential linearly depends on pH in the range of 3.15–9.13 according to the following equation: E_p (V) = –0.059 pH + 1.1298, with R^2 = 0.9954. The slope of –59.0 mV pH^{-1} indicates that electron transfer is accompanied by an equal number of protons during the electrochemical oxidation reaction of VAN on PPy_{ov-ox}/GCE.

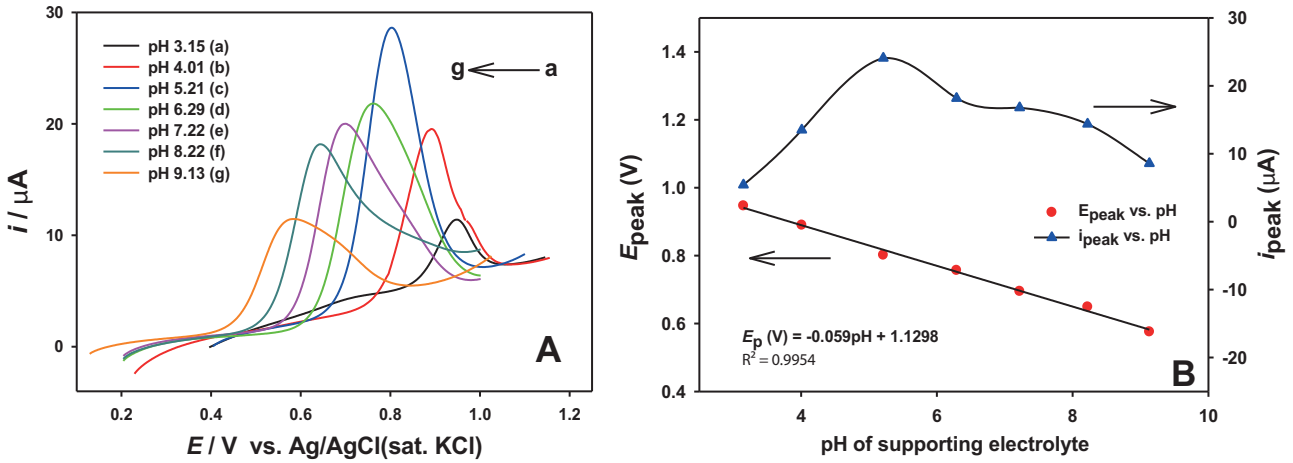

Figure 6. A) Linear voltammograms for 0.1 mmol L^{-1} VAN on PPy_{ov-ox}/GCE in different buffer solutions with pH values of 3.15, 4.01, 5.20, 6.29, 7.22, 8.22, and 9.13. B) Influence of pH on the oxidation peak current and potential of VAN.

2.4. The effect of scan rate on VAN electrooxidation

In order to investigate whether the oxidation behavior of VAN was due to VAN diffusing in solution or adsorbing on PPy_{ov-ox}/GCE, the cyclic voltammograms of 0.1 mmol L^{-1} VAN at different scan rates (0.005–0.200 V s^{-1}) were recorded in pH 5.2 buffer solution on PPy_{ov-ox}/GCE (Figure 7A). The results showed that the peak current (i_{pa}) varies linearly with the square root of the scan rate ($\nu^{1/2}$) (Figure 7B). The linearity of the $i_{pa} - \nu^{1/2}$ plot indicates diffusion-controlled behavior during the electrode reaction of VAN oxidation on PPy_{ov-ox}/GCE.

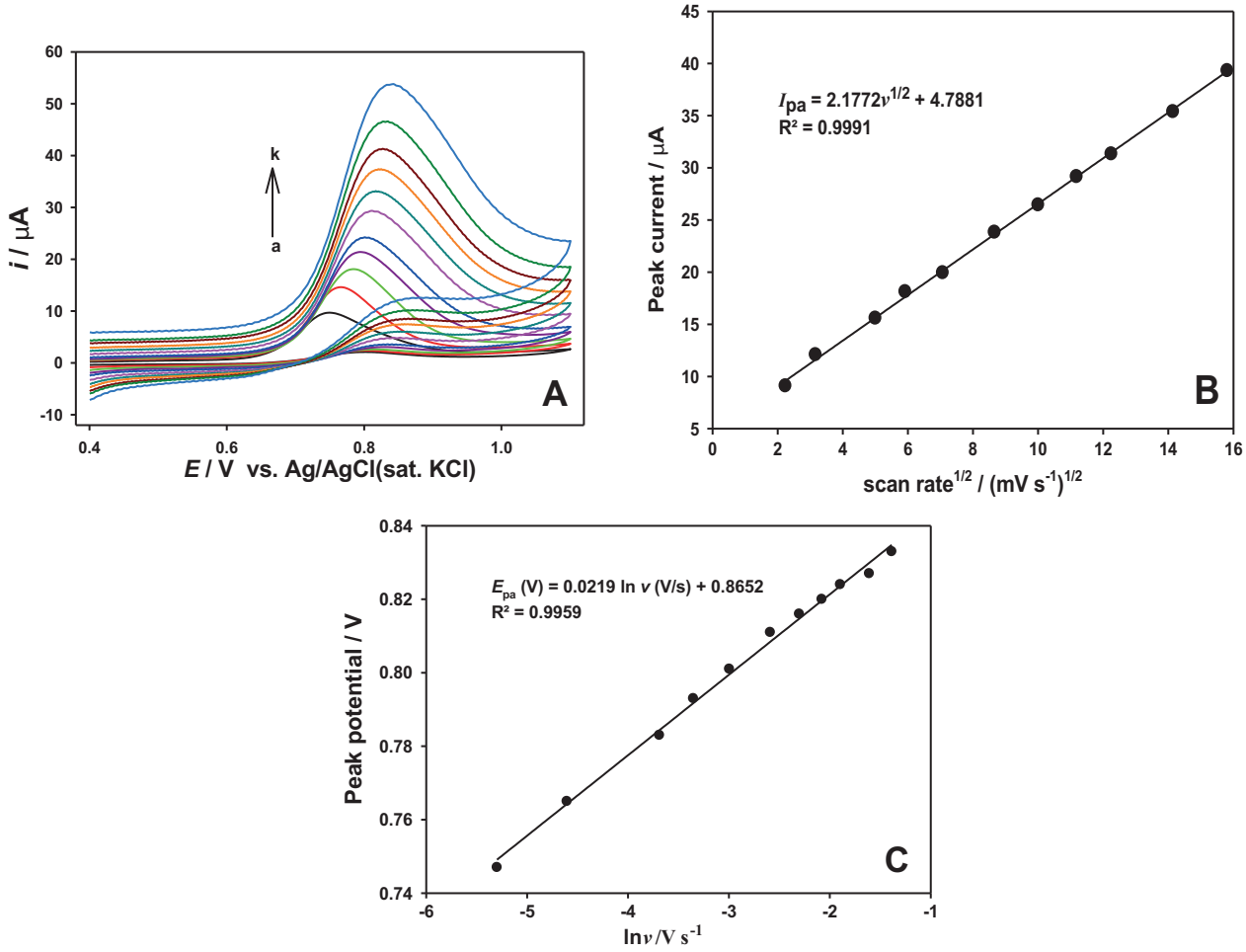

Figure 7. A) Cyclic voltammograms of 0.1 mmol L^{-1} VAN in pH 5.2 buffer solution with various scan rates (5.0, 10.0, 25.0, 35.0, 50.0, 75.0, 100.0, 125.0, 150.0, 200.0, 250.0 mV s^{-1}). B) The I_{pa} vs. v plot. C) The E_{pa} vs. ln$v$ plot.

The oxidation peak potential of VAN shifted to more positive potential with the increasing of the scan rate of potential scan. A linear relationship formed between the oxidation potentials (E_p) and ln$v$. The regression equation was found as $E_p = 0.0219 \ln v + 0.8652$ ($R^2 = 0.9959$) (Figure 7C). According to Laviron's theory[39] for an irreversible electrode process, E_p is defined by the following equation:

$$E_p = E^{0'} + \frac{RT}{anF} lnv \tag{2}$$

Here, E_p is the peak potential (V vs. Ag/AgCl), $E^{0'}$ is the formal potential (V vs. Ag/AgCl), R is the universal gas constant (8.314 J K^{-1} mol^{-1}), T is the temperature (K), α is the charge transfer coefficient for the oxidation step, $n$is the number of electrons involved in the rate-determining step, and F is the Faraday constant (96,485 C mol^{-1}). The slope of the E_p-ln v line can be expressed as RT/anF. According to Bard and Faulkner,[40] E_p positively shifted by an amount of 1.15 RT/αF (or $30/\alpha$ mV at 25 °C) for each tenfold increase in v. Thus, the value of α can be calculated from this equation as 0.588. The number of electrons (n) transferred in the electrooxidation of VAN was found to be 1.99 (approximately equal to 2), so the proposed electrooxidation mechanism of VAN on the PPy_{ov-ox}/GCE surface may be expressed with the following Scheme, in which two electrons and two protons take part in the electrode process.

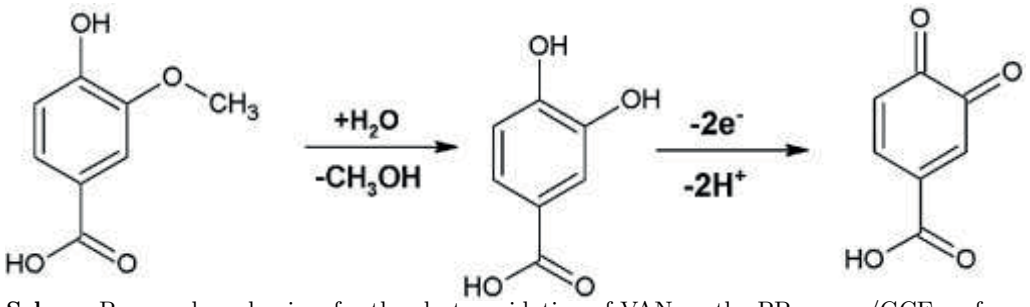

SchemeProposed mechanism for the electrooxidation of VAN on the PPy_{ov-ox}/GCE surface.

2.5. The calibration curves for VAN determination on PPy_{ov-ox}/GCE

Under the optimized working conditions, differential pulse voltammetry (DPV) studies were carried out to evaluate the sensitivity of the chemical sensor with various VAN concentrations on PPy_{ov-ox}/GCE in pH 5.2 buffer solution (Figures 8A and 8B). The obtained calibration curves in the inset of Figures 8A and 8B clearly indicate that the oxidation peak current is linearly proportional to VAN concentrations in the ranges of 3.20 $\times$ 10^{-8} to 1.50 $\times$ 10^{-6} mol L^{-1} and 3.0 $\times$ 10^{-6} to 1.50 $\times$ 10^{-4} mol L^{-1}. The linear equations obtained from the calibration curve are i_p (μA) = 1.3785 C_{VAN} (μmol L^{-1}) + 0.0148 (R^2 = 0.9990) and i_p (μA) = 0.1915 C_{VAN} (μmol L^{-1}) + 3.4974 (R^2 = 0.9965), respectively. The limit of detection (LOD) value for VAN on PPy_{ov-ox}/GCE was calculated to be 1.21 $\times$ 10^{-8} mol L^{-1} using the equation LOD = 3.3σ/m, where σ is the standard deviation of the response for blank solution and m is the slope of the calibration curve. The relative standard deviations (RSDs) of the calibration curve slope and intercept value (n = 3) were also calculated as 2.1% and 1.1%, respectively. These results showed that PPy_{ov-ox}/GCE has higher sensitivity and lower detection limit than some developed sensors in previously published studies, as illustrated by the values in Table 1.

2.6. Selectivity, reproducibility, repeatability, robustness, ruggedness, and long-term stability of PPy_{ov-ox}/GCE

To investigate the selectivity of the developed method, an interference study was performed under optimized conditions in the presence of various interferences such as organic and inorganic compounds. It was found that K^+, Cl^-, NO_3^-, Na^+, SO_4^{2-}, Zn^{2+}, Al^{3+}, Mg^{2+}, $Fe^{3+,}$ Pb^{2+}, glucose, sucrose, oxalic acid, citric acid, benzoic acid, tartaric acid, and caffeic acid showed no obvious interference to the determination of 5.0 $\times$ 10^{-6}

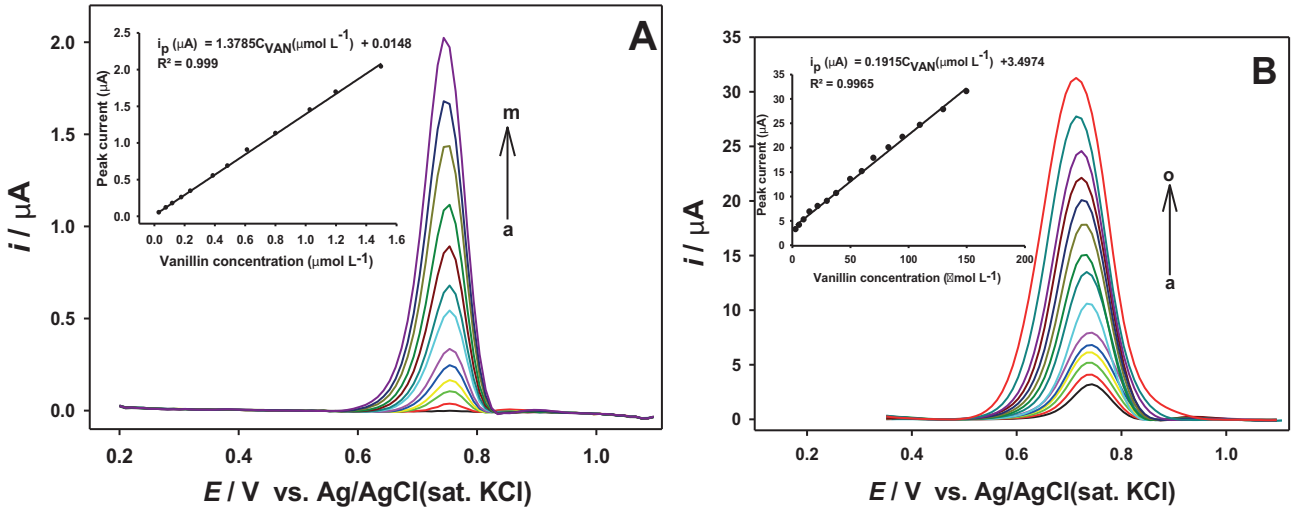

Figure 8. DPVs of PPy_{ov-ox}/GCE in different concentrations of vanillin solutions in pH 5.2 buffer solution. A) a–m: 0, 3.2×10^{-8}, 7.8×10^{-8}, 1.2×10^{-7}, 1.8×10^{-7}, 2.4×10^{-7}, 3.89×10^{-7}, 4.85×10^{-7}, 6.15×10^{-7}, 8.02×10^{-7}, 1.03×10^{-6}, 1.2×10^{-6}, 1.5×10^{-6} mol L^{-1}. Insert: Calibration curve. B) a–o: 3.0×10^{-6}, 6.0×10^{-6}, 1.0×10^{-5}, 1.5×10^{-5}, 2.2×10^{-5}, 3.0×10^{-5}, 3.8×10^{-5}, 5.0×10^{-5}, 6.0×10^{-5}, 7.0×10^{-5}, 8.3×10^{-5}, 9.5×10^{-5}, 1.1×10^{-4}, 1.3×10^{-4}, 1.5×10^{-4}. Insert: Calibration curve.

Table 1. Comparison of some characteristics of the different electrodes for the determination of VAN.

Electrode	Mode	LR (μmol L^{-1})	LOD (μmol L^{-1})	Ref.
CDA/Au-AgNPs/GCE	Amperometric measurement	0.2–50.0	0.04	[2]
Graphene/GCE	DPV	0.06–48.0	0.056	[41]
BDDE	DPAdSV	3.3–98.0	0.16	[11]
Au-Pd/graphene/GCE	DPV	0.1–7.0 10.0–40.0	0.02	[9]
AgNPs/GN/GCE	SWV	2.0–100.0	0.332	[22]
AuNP-PAH/GCE	SWV	0.90–15.0	0.055	[20]
EMDG/GCE	DPV	0.10–45.0	0.032	[8]
CPB/CNF/GCE	DPV	0.50–75.0 75.0–750.0	0.14	[4]
CoSNR-GCE	DPV	0.5–56.0	0.07	[21]
PPy_{ov-ox}/GCE	DPV	0.032–1.50 3.0–150.0	0.012	This study

CDA/Au-AgNPs/GCE: Cellulose diacetate-Au-Ag alloy-glassy carbon electrode; DPV: differential pulse voltammetry; BDDE: boron-doped diamond electrode; DPAdSV: differential pulse adsorptive stripping voltammetry; Arg-G/GCE: arginine functionalized graphene modified GCE; AgNPs/GN/GCE: Ag nanoplates graphene modified GCE; SWV: square wave voltammetry; AuNP-PAH/GCE: Au nanoparticles stabilized in poly(allylaminehydochloride) modified GCE; EMDG/GCE: electrolytic manganese dioxide-graphene modified GCE; CPB/CNF/GCE: cationic cetylpyridium bromide-carbon nanofibers modified GCE; CoSNR-GCE: cobalt sulfide nanorods modified GCE.

mol L^{-1} VAN even when present 1000 times in excess, with deviations below 5.0%. On the other hand, the presence of ethyl vanillin in the same concentration with VAN showed strong interference due to a similar oxidation potential of this compound. Another positive difference was observed for the VAN oxidation peak current in the presence of more than 500-fold amounts of Cu^{2+} or Mn^{2+} ions. Hence, the selectivity of the

suggested voltammetric method for VAN determination is similar to that of other developed sensors in the literature. In order to evaluate the analytical parameters of the polymer film electrode for VAN determination, the RSDs were obtained from the DPV analyses for interday (n = 10) and intraday (n = 10) sampling intervals with PPy_{ov-ox}/GCE for two VAN concentrations. The interday RSD values for 5.0×10^{-7} and 5.0×10^{-6} mol L^{-1} VAN were 2.6% and 3.31%, respectively, and the intraday RSD values for these two concentrations were 3.56% and 4.76%, respectively. These RSD values indicate that the PPy_{ov-ox}/GCE has good reproducibility. The repeatability of the PPy_{ov-ox}/GCE was investigated under optimized conditions for 5.0×10^{-6} mol L^{-1} VAN in pH 5.2 with 20 DPV measurements. The RSD value of subsequent measurements was calculated as 2.9%.

The robustness of the developed method is the ability to remain unaffected by small changes in its operational parameters. Robustness tests were performed with small changes of buffer solution pH (pH 5.0 and pH 5.4), scan rate (18.0 mV s^{-1} and 22.0 mV s^{-1}), and amplitude (48 mV and 52 mV) of the DPV technique with PPy_{ov-ox}/GCE (Table 2) in the presence of 6.0 μmol L^{-1} VAN. Only one parameter was changed in each experiment. As can be seen from Table 2, the RSD% and recovery% values were not significantly affected by these variations. Minor changes in the pH of the buffer solution, scan rate, and amplitude values of the DPV technique did not have any important effect on the peak current and peak potential of VAN. Consequently, the results indicated that the developed method was reliable for the assay of VAN in the various samples and hence it could be considered robust.

Table 2. The robustness data of the proposed DPV method with PPy_{ov-ox}/GCE.

Added concentration (μmol L^{-1})	Found concentration (μmol L^{-1})	RSD%	Recovery%
Optimum conditions (6.0 μmol L^{-1})	6.11	0.17	101.83
pH 5.0	6.20	0.16	103.33
pH 5.4	5.91	0.59	98.50
Scan rate 18 mV s^{-1}	5.95	0.68	99.17
Scan rate 22 mV s^{-1}	6.18	0.85	103.00
Amplitude 48 mV	5.98	0.51	99.66
Amplitude 52 mV	6.30	0.92	105.00

Ruggedness is the degree of reproducibility of the assay results obtained by the analysis of the same sample under a variety of normal test conditions, such as different laboratories and analysts on different days. The ruggedness of the proposed method was evaluated by applying the developed procedures to assay 5.0 μmol L^{-1} of VAN standard solution in the method using the same instrument by two different analysts under the optimized conditions on different days. The obtained results were compared by means of the F-test. The results were found to be reproducible because there was no significant difference between the results obtained by the two analysts, which are experimental value F_t and theoretical value F_c ($F_c = 19.00 > F_t = 3.21$, $P > 0.05$, n = 3). The developed method could be said to be rugged.

The long-term stability of the modified electrode was investigated by examining the peak current response of 5.0×10^{-6} mol L^{-1} VAN, and the modified electrode was stored in 0.1 mol L^{-1} at pH 5.2 buffer solution at room temperature during the stability measurements. The current response of the electrode for VAN retained about 97.2% of its initial current after 20 days, which shows that the stability of the modified electrode is good enough for use in long-life voltammetric sensors.

2.7. VAN determination in commercial food products

In order to evaluate the applicability of the developed method, the PPy$_{ov-ox}$/GC electrode was used to analyze VAN in three commercial products including biscuit, cake, and wafer samples pretreated according to the sample preparation method in Section 3.3 under optimized conditions. The standard addition method was applied to determine the content of VAN in these samples. The contents of VAN in real samples and the recovery results are listed in Table 3. The contents of VAN in biscuit, cake, and wafer samples were found to be 83.38 μg/g, 58.12 μg/g, and 108.64 μg/g, respectively. The recoveries for the added standards ranged between 94.03% and 104.23%. As can be seen from these results, the prepared PPy$_{ov-ox}$/GCE can be successfully used for the determination of VAN in real samples.

Table 3. Determination of VAN at PPy$_{ov-ox}$/GCE in different food samples (n = 3).

Samples	Added (μmol L^{-1})	Found (μmol L^{-1})	Recovery (%)	RSD (%)
Biscuit	0	2.74	-	2.2
	6.0	8.52	97.48	2.6
	8.0	10.98	102.23	3.5
	10.0	11.98	94.03	4.1
Cake	0	1.91	-	3.1
	6.0	7.62	96.33	3.7
	8.0	10.20	102.93	3.1
	10.0	12.01	100.83	2.8
Wafer	0	3.57	-	4.1
	6.0	9.78	102.19	4.2
	8.0	12.06	104.23	3.7
	10.0	13.07	96.31	3.5

The obtained results for determination of vanillin in three different samples, biscuit, cake, and wafer, by DPV technique were compared with the high-performance liquid chromatography (HPLC) technique. The statistical comparison of DPV analysis results with HPLC analysis results was performed using the t-test and F-test and the results are shown in Table 4. All experimental values (t_t and F_t) did not exceed the theoretical ones (t_c and F_c) ($P > 0.05$), which revealed that there is no significant difference between the performance of the two methods.

2.8. Conclusions

We have successfully fabricated a novel, simple, and cheap electrochemical sensor for VAN determination based on an overoxidized poly(pyrrole) film-modified GCE. The PPy$_{ov-ox}$/GCE displayed excellent electrocatalytic properties in terms of fast current response, low detection limit, good selectivity, reproducibility, and long-term stability towards the electrochemical oxidation of VAN. DPV studies showed that the peak currents increased linearly within the ranges of 0.032–1.500 μmol L^{-1} and 3.00–150.00 μmol L^{-1} with a detection limit of 0.012 μmol L^{-1}. Furthermore, this modified electrode has been successfully applied to the determination of VAN in three commercial products including biscuit, cake, and wafer samples. These results indicate that the PPy$_{ov-ox}$/GCE may be applicable to other related food products.

Table 4. Comparative determination of VAN in commercial food product by the proposed DPV method and the HPLC method (n = 3).

Sample	Proposed DPV method (μg/g VAN)	Comparison method (HPLC) (μg/g VAN)
Biscuit	$\bar{x} = 83.380 \pm 0.029$	$\bar{x} = 83.382 \pm 0.12$
	RSD% = 0.034	RSD% = 0.143
	$t_c = 2.77 > t_t = 0.06$, $P > 0.05$	
	$F_c = 19.0 > F_t = 17.9$, $P > 0.05$	
Cake	$\bar{x} = 58.12 \pm 0.493$	$\bar{x} = 58.12 \pm 0.497$
	RSD% = 0.849	RSD% = 0.855
	$t_c = 2.77 > t_t = 0.001$, $P > 0.05$	
	$F_c = 19.0 > F_t = 1.014$, $P > 0.05$	
Wafer	$\bar{x} = 108.640 \pm 0.467$	$\bar{x} = 108.644 \pm 0.578$
	RSD% = 0.429	RSD% = 0.532
	$t_c = 2.77 > t_t = 0.014$, $P > 0.05$	
	$F_c = 19.0 > F_t = 1.53$, $P > 0.05$	

Found = $\bar{x} = mean \pm standard\,error$; RSD% = relative standard deviation.

3. Experimental

3.1. Reagents and apparatus

All the reagents were of analytical grade and all the solutions were prepared using ultrapure water obtained from a Millipore Milli-Q System (18.2 Ω). Pyrrole (Py) was distilled three times until a colorless liquid was obtained, and the monomer was then stored in a refrigerator at 4.0 °C. Sodium dodecyl sulfate (SDS), CH_3COOH, $NaCH_3COO$, $H_3C_6H_5O_7$, $Na_3C_6H_5O_7$, NaH_2PO_4, Na_2HPO_4, H_3BO_3, $NaBO_2.4H_2O$, NaOH, and ethanol were purchased from Sigma-Aldrich or Merck. All experiments were performed at room temperature. Pure nitrogen was used to remove oxygen from the solution. Electrochemical measurements were performed using an Autolab PGSTAT 302N Electrochemical Analyzer. GCE, Ag/AgCl (sat. KCl), and Pt wire were used as the working, reference, and counter electrodes, respectively, for all experiments. Electrochemical measurements were carried out with EIS, CV, and DPV techniques. The morphological, electrical, and chemical properties of polymer film electrodes were investigated by SEM (Carl Zeiss 300 VP), EIS (Autolab PGSTAT 302N Electrochemical Analyzer), and XPS (Thermo Scientific K-Alpha), respectively. An HPLC analysis system (Agilent-1100) equipped with a UV detector was used for HPLC analysis for VAN. Chromatographic separation was carried out on a Phenomenex HyperClone 3 μm ODS (C18) 150 $\times$ 4.6 mm column.

3.2. Preparation of overoxidized poly(pyrrole) film GCE

Prior to the electropolymerization procedure, the GCE was cleaned by polishing with a 0.5 μm aqueous alumina slurry on microcloth pads to obtain a mirror-like finish. The electrode was sonicated for 3 min each in ethanol and pure water, respectively. A PPy film was coated on the GCE surface by cyclic voltammetry according to the procedure described in our previous work.[42] Briefly, the PPy film was electrodeposited on the GCE surface in 0.1 mol L^{-1} SDS containing 0.1 mol L^{-1} pyrrole with the cycling potential between –0.35 and 0.85 V vs. Ag/AgCl at a scan rate of 20 mV s^{-1} for seven cycles. In the electrochemical polymerization experiments of the pyrrole, SDS acts as a unique dopant and significantly changes the microscopic and macroscopic properties of

the polymer structure. Moreover, using SDS decreases the polymerization potential, allowing the microstructure polymer. The electroreduction removes the SDS anion from the polymer backbone. This leads to changes in the morphology of the poly(pyrrole) structure, which enhances the polymer's specific capacitance.[43,44] After the electropolymerization step, the polymer film electrode (PPy/GCE) was rinsed thoroughly with ultrapure water for further application. Then the PPy/GCE was moved into 0.1 M NaOH solution for electrochemical overoxidation of the PPy film at +1.0 V for 100 s. The obtained electrode was ready for use after a final wash with ultrapure water and denoted as PPy_{ov-ox}/GCE. The PPy_{ov-ox}/GCE was prepared before each voltammetric study of the whole effect of pH and effect of scan rate on VAN oxidation experiments. The DPV studies were carried out with the same modified electrode.

3.3. Preparation of commercial food samples for vanillin determination

Various commercial food products such as biscuits, cakes, and wafers were bought from a market. VAN was extracted from these food products as follows. First, the food samples were ground in a mortar with a pestle until powder samples were obtained. About 0.5 g of powdered biscuit, cake, and wafer samples were weighed and transferred into tubes. Ethanol (10.0 mL) was added to the tubes. The mixture was mechanically shaken for 90 min. Centrifugations of the samples were then carried out at 4000 rpm for 20 min. Finally, the clear part of the solution in the tube was used for vanillin determination.

References

1. Bettazzi, F.; Palchetti, I.; Sisalli, S.; Mascini, M. A. *Anal. Chim. Acta* **2006**, *55*, 134-138.
2. Zheng, D.; Hu, C.; Gan, T.; Dang, X.; Hu, S. *Sens. Actuators B* **2010**, *148*, 247-252.
3. Filik, H.; Avan, A. A.; Mümin, Y. *Food Anal. Methods* **2017**, *10*, 31-40.
4. Ziyatdinova, G.; Kozlova, E.; Ziganshina, E.; Budnikov, H. *Monatsh. Chem.* **2016**, *147*, 191-200.
5. Wang, X.; Luo, C.; Li, L.; Duan, H. *RSC Adv.* **2015**, *5*, 92932-92939.
6. Sun, J.; Gan, T.; Wang, K.; Shi, Z.; Li, J.; Wang, L. *Anal. Methods* **2014**, *6*, 5639-5646.
7. Luo, S.; Liu, Y. *Int. J. Electrochem. Sci.* **2012**, *7*, 6396-6405.
8. Liu, Y.; Liang, Y.; Lian, H.; Zhang, C.; Peng, J. *Int. J. Electrochem. Sci.* **2014**, *10*, 4129-4137.
9. Shang, L.; Zhao, F.; Zeng, B. *Food Chem.* **2014**, *151*, 53-57.
10. Xinying, M. A. *Int. J. Electrochem. Sci.* **2014**, *9*, 3181-3189.
11. Yardim, Y.; Gulcan, M.; Şenturk, Z. *Food Chem.* **2013**, *141*, 1821-1827.
12. Sostaric, T.; Boyce, M. C.; Spickett, E. E. *J. Agric. Food. Chem.* **2000**, *48*, 5802-5807.
13. De Jager, L. S.; Perfetti, G. A.; Diachenko, G. W. *Food Chem.* **2008**, *107*, 1701-1709.
14. Waliszewski, K. N.; Pardio, V. T.; Ovando, S. L. *Food Chem.* **2006**, *101*, 1059-1062.
15. Lamprecht, G.; Pichlmayer, F.; Schmid, E. R. *J. Agric. Food. Chem.* **1994**, *42*, 1722-1727.
16. Ni, Y.; Zhang, G.; Kokot, S. *Food Chem.* **2005**, *89*, 465-473.
17. Ohashi, M.; Omae, H.; Hashida, M.; Sowa, Y.; Imai, S. *J. Chromatogr. A* **2007**, *1138*, 262-267.
18. Wu, W.; Wang, H.; Yang, L.; Zhao, F.; Zeng, B. *Int. J. Electrochem. Sci.* **2016**, *11*, 6009-6022.
19. Deng, P.; Xu Z.; Zeng, R.; Ding, C. *Food Chem.* **2015**, *180*, 156-163.
20. Silva, T. R.; Brondani, D.; Zapp, E.; Vieira, C. *Electroanalysis* **2015**, *27*, 465-472.
21. Sivakumar, M.; Sakthivel, M.; Chen, S. M. *J. Colloid Interface Sci.* **2017**, *490*, 719-726.

22. Huang, L.; Hou, K.; Jia, X.; Pan, H.; Du, M. *Mater. Sci. Eng. C* **2014**, *38*, 39-45.
23. Becerik, İ.; Kadırgan, F. *Turk. J. Chem.* **2001**, *25*, 373-380.
24. Çolak, Ö.; Arslan, F. *Turk. J. Chem.* **2015**, *39*, 84-95.
25. Can, M.; Pekmez, K.; Pekmez, N.; Yıldız, A. *Turk. J. Chem.* **1998**, *22*, 47-53.
26. Majidi, M. R.; Jouyban, A.; Asadpour-Zeynali, K. *J. Electroanal. Chem.* **2006**, *589*, 32-37.
27. Pihel, K.; Walker, Q. D.; Wightman, R. M. *Anal. Chem.* **1996**, *68*, 2084-2089.
28. Li, J.; Lin, X. Q. *Anal. Chim. Acta* **2007**, *596*, 222-230.
29. Haghighi, B.; Tabrizi, M. A. *Colloids Surf. B* **2013**, *103*, 566-571.
30. Bai, J.; Ndamanisha, J. C.; Liu, L.; Yang, L.; Guo, L. *J. Solid State Electrochem.* **2010**, *14*, 2251-2256.
31. Song, M. J.; Hwang, S. W.; Whang, D. *Talanta* **2010**, *80*, 1648-1652.
32. Konopka, S. J.; McDuffie, B. *Anal. Chem.* **1970**, *42*, 1741-1746.
33. Fuge, G. M.; Rennick, C. J.; Pearce, S. R. J.; May, P. W.; Ashfold, M. N. R. *Diamond Relat. Mater.* **2003**, *12*, 1049-1054.
34. Palmisano, F.; Malitesta, C.; Centonze, D.; Zambonin, P. G. *Anal. Chem.* **1995**, *67*, 2207-2211.
35. Süzer, Ş.; Birer, Ö.; Sevil, U. A.; Güven, O. *Turk. J. Chem.* **1998**, *22*, 59-65.
36. Jaramillo, A.; Spurlock, L. D.; Young, V.; Brajter-Toth, A. *Analyst* **1999**, *124*, 1215-1221.
37. Malitesta, C.; Losito, I.; Sabbatini, L.; Zambonin, P. G. *J. Electron. Spectrosc. Relat. Phenom.* **1995**, *76*, 629-634.
38. Idla, K.; Talo, A.; Niemi, H. E. M.; Forsén, O.; Yläsaari, S. *Surf. Interface Anal.* **1997**, *25*, 837-854.
39. Laviron, E. *J. Electroanal. Chem.* **1979**, *100*, 263-270.
40. Bard, A. J.; Faulkner, L. R. *Electrochemical Methods Fundamentals and Application*, 2nd ed.; Wiley: New York, NY, USA, 2004.
41. Peng, J.; Hou, C.; Hu, X. *Int. J. Electrochem. Sci.* **2012**, *7*, 1724-1733.
42. Ulubay, Ş.; Dursun, Z. *Talanta* **2010**, *80*, 1461-1466.
43. Nikoofard, H.; Kalantar, Z.; Omidian, M. *Res. Rev. Electrochem.* **2014**, *5*, 101-108.
44. El-Enany, G.; El-Maksoud, S.A.A.; Hamouda, R.; El-Seify, F. *Der Pharma Chemica* **2016**, *8*, 156-162.